STUDIES OF ULTRASHORT THz PULSES AT DELTA*

P. Ungelenk†, C. Mai‡, L.-G. Böttger, S. Hilbrich, M. Höner, H. Huck,
M. Huck, S. Khan, A. Meyer auf der Heide, R. Molo, H. Rast, A. Schick,
Center for Synchrotron Radiation (DELTA), TU Dortmund University, Dortmund, Germany
N. Hiller, V. Judin, J. Raasch, P. Thoma,
IPS, ANKA and IMS, Karlsruhe Institute of Technology (KIT), Karlsruhe, Germany
S. Bielawski, C. Evain, M. Le Parquier, E. Roussel, C. Szwaj,
PhLAM/CERLA, Université Lille 1, Villeneuve d'Ascq, France

Abstract

At DELTA, a 1.5-GeV electron storage ring operated as a light source by the Center for Synchrotron Radiation at the TU Dortmund University, coherent ultrashort THz pulses are routinely generated by density-modulated electron bunches. Tracking simulations as well as experimental studies using ultrafast THz detectors and an FT-IR spectrometer aim at understanding the turn-by-turn evolution of the density modulation after an initial laser-electron interaction. Furthermore, intensity-modulated laser pulses are applied to create narrow-band THz radiation. This setup is part of the new short-pulse facility based on coherent harmonic generation.

INTRODUCTION

DELTA is a 1.5-GeV electron storage ring operated as a light source by the Center for Synchrotron Radiation at the TU Dortmund University. A new short-pulse facility based on the coherent harmonic generation (CHG) principle [1] is in operation since 2011 [2–4]. As shown in Fig. 1, an ultrashort laser pulse (red) interacts with a short section of the electron bunch (green, not to scale) in a first undulator, thereby introducing a periodic energy modulation. Using a magnetic chicane, the energy modulation is converted into a series of microbunches, which emit coherent VUV radiation at harmonics of the original laser wavelength in a second undulator. While passing through subsequent bending magnets, electrons with an energy deviation move on dispersive orbits with different path lengths, leaving a dip on the sub-millimeter scale. This density modulation gives rise to coherent THz radiation [5], which is emitted in a bending magnet and extracted by a dedicated THz beamline [6].

The intensity of the coherent THz radiation is routinely used as a measure to find, optimize and maintain the laser-electron overlap, e.g. for stable operation of the CHG-based VUV source. Other applications of the THz radiation include bunch profile measurements [7]. For future user experiments, it is vital to further understand and optimize the mechanism behind the generation of the THz pulses. Recent studies address the turn-by-turn evolution of the density modulation as well as means to create narrow-band THz radiation.

* Work supported by the DFG (INST 212/236-1 FUGG), the BMBF (05K13PEC), and the state of NRW.
† peter.ungelenk@tu-dortmund.de
‡ carsten.mai@tu-dortmund.de

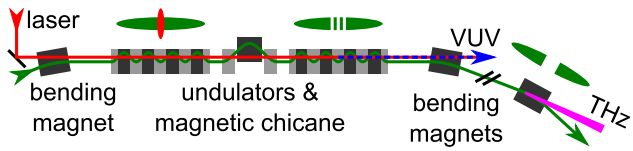

Figure 1: Sketch of the facility for ultrashort VUV and THz pulses at DELTA (see text for details).

TURN-BY-TURN EVOLUTION OF THE THz PULSES

During operation of the short-pulse facility, the storage ring is filled with either a single bunch or a hybrid pattern (multi-bunch train plus one high-current single bunch). Due to the revolution frequency of 2.6 MHz and the laser repetition rate of 1 kHz, a laser-electron interaction occurs only at every 2600th revolution.

Ultrafast THz Detectors at DELTA

Limited by a rather slow InSb hot-electron bolometer (350 ns rise time vs. 384 ns revolution time), early measurements could only indicate coherent THz pulses integrated over several revolutions after the laser-electron interaction [6]. The survival of the density modulation over several revolutions, which has also been observed at other machines (e.g. [5]), could be confirmed in 2012 [8] using a NbN-based hot-electron bolometer from the ANKA synchrotron radiation facility at Karlsruhe Institute of Technology (KIT) with a response time of less than 160 ps (FWHM) [9, 10]. Recently, a new detector type based on the high-temperature superconductor $YBa_2Cu_3O_7$ ('YBCO') with an ultrafast response time of less than 17 ps (FWHM) has been developed by the Institute of Micro- and Nanoelectronic Systems (IMS) at KIT [11, 12] and was tested at DELTA in June 2013.

Figure 2 shows THz signals recorded with these three detector types under similar conditions. After the initial laser-electron interaction at about $t = -100$ ns, an immediate response from the YBCO detector occurs at $t = 0$, followed by a weak, delayed response from the slower InSb detector. Originating from the first pass of the electron bunch before completing a full revolution, this is referred to as 'turn 0'. For the NbN measurement, an attenuator suppressing the turn-0 and reducing the turn-1 signal was used, thereby allowing a more sensitive detection of turn 2 and following turns. After a full revolution in the storage ring, all detectors show highest

ISBN 978-3-95450-132-8

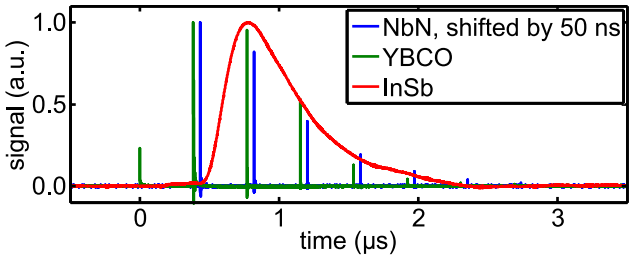

Figure 2: Normalized signals from the NbN, the YBCO and the InSb detector. For better visibility, the NbN trace is shifted by 50 ns.

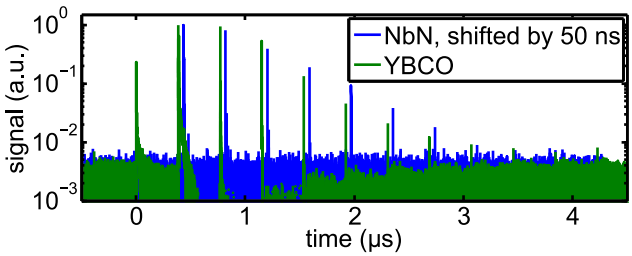

Figure 3: Normalized signals from the NbN and YBCO detector on a semi-logarithmic scale. For better visibility, the NbN trace is shifted by 50 ns.

intensity at the turn-1 signal. Afterwards, the intensities drop exponentially. The spectrum of the THz pulses is expected to be shifted to lower frequencies from turn to turn (see simulation results below). Therefore, the intensities are not only related to the decaying amplitude of the density modulation, but also to the changing overlap between the emission spectrum and the respective detector sensitivity.

Using a semi-logarithmic scale (Fig. 3), coherent signals from at least nine revolutions (turn 0 to 8) can be seen on the YBCO and NbN traces.

In contrast to InSb and NbN, YBCO features a non-bolometric, electric field detection mechanism for photon energies below the superconducting energy gap [13, 14], which is presumably exceeded by the broad-band turn-0 signal (1.5 THz to 3.5 THz FWHM, see spectra below). Hence, the turn-0 signal shows a slow bolometric tail over more than 10 ns (Fig. 4, turn 0), which does not appear, e.g., in the turn-2 and turn-4 signals. The transition between the

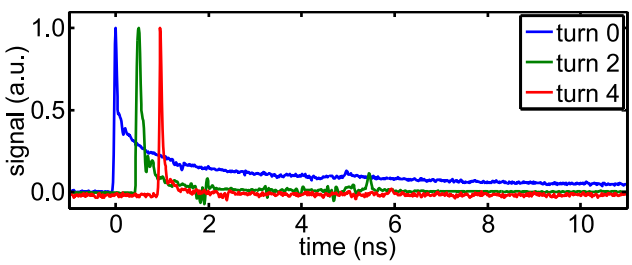

Figure 4: Normalized single-turn signals from the YBCO detector. For better visibility, the turn-2 and turn-4 traces are shifted by 0.5 ns and 1 ns, respectively.

bolometric and the electric field detection regime will be analyzed further in the near future using narrow-band THz radiation (see below).

Tracking Simulations

Simulations of the laser-electron interaction and the electron trajectories over subsequent revolutions have been performed using a self-developed software [15] and `elegant` [16]. Figure 5 shows two examples for longitudinal density profiles as well as the evolution of the dip width. The narrow dip with adjacent peaks for turn $n = 0$ is significantly flattened and broadened over the following revolutions due to longitudinal dispersion and path length differences caused by the natural energy spread and the transverse spatial and angular distribution of the electrons.

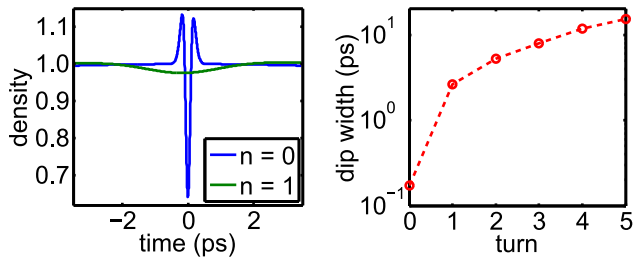

Figure 5: Examples of the simulated longitudinal electron density for turn $n = 0$ and 1 (left) and width of the dip (FWHM) versus turn number (right).

A Fourier transformation of the longitudinal electron density yields the coherent THz spectrum, which reaches from 1.5 THz to 3.5 THz (FWHM) for $n = 0$ and is shifted towards lower frequencies for the following revolutions (Fig. 6). This is in good agreement with experimental results, e.g., the measured turn-0 spectra (Fig. 7) or the weak turn-0 InSb response (Fig. 2), as the InSb bolometer is only sensitive below 1 THz. In addition, the finite bunch length of about 100 ps (FWHM) leads to a coherent signal reaching from 0.5 GHz to 5 GHz, which is just below the vacuum chamber cutoff and does not propagate through the beamline.

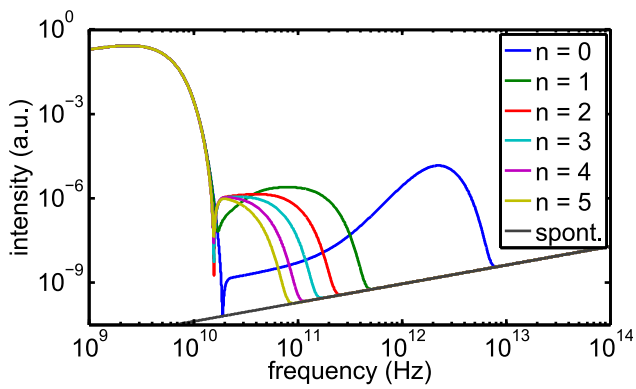

Figure 6: Simulation of the THz spectrum for revolutions $n = 0$ to 5 after an initial laser-electron interaction. For reference, the spontaneous incoherent bending magnet spectrum is also shown.

ISBN 978-3-95450-132-8

DETECTION AND MANIPULATION OF THE THz SPECTRA

THz spectra are measured using a vacuum FT-IR spectrometer. Here, the employed beam splitter presents a low frequency cutoff (10% of peak) at 1.1 THz, and a z-cut quartz window separating the THz beamline from the storage-ring vacuum leads to a high frequency cutoff at 6.5 THz.

Broad-Band THz Pulses

Figure 7 shows the form factor $g^2(\nu)$, which is the squared Fourier transform of the longitudinal electron density, times the number of electrons N_e in the single bunch. It is obtained from the measured coherent spectrum $I_1(\nu)$ and the spontaneous spectrum $I_0(\nu)$ according to [8]

$$N_e \cdot g^2(\nu) = 2600 \cdot \frac{I_1(\nu) - I_0(\nu)}{I_0(\nu)}. \quad (1)$$

The numerical factor of 2600 takes into account the number of incoherent bunch signals which are detected between two coherent signals.

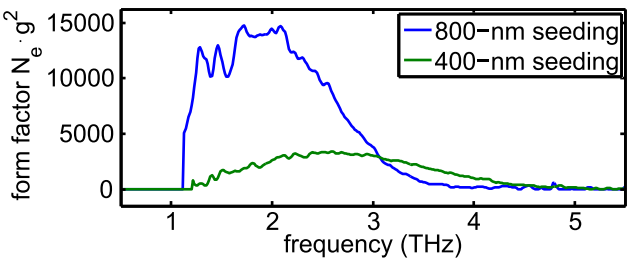

Figure 7: Coherent THz spectra (number of electrons N_e times form factor g^2) recorded using different seeding laser wavelengths.

Until the beginning of 2014, seeding was only possible with 400 nm due to a fixed, CHG-optimized setup using a second-harmonic generation unit in the laser laboratory and corresponding mirrors in the seeding beamline. Now, quick switching to seeding with the fundamental 800 nm of the Ti:sapphire laser system is possible, which leads to about 50 % more pulse energy and, presumably, to slightly shorter pulses and less wavefront aberrations. This is reflected by a slightly broader spectrum at lower frequencies (Fig. 7, showing a bandwidth (FWHM) of 2.6 THz at 800 nm vs. 2.0 THz at 400 nm) with a much higher form factor of $N_e \cdot g^2 \approx 15000$ vs. 3400, recorded at equal bunch current of about 12 mA.

Narrow-Band THz Pulses

Narrow-band radiation pulses in the sub-THz range have been generated at the synchrotron light source UVSOR in Japan for several years [17, 18] using the so-called chirped pulse beating (CPB) technique [19]. Here, uncompressed, linearly chirped pulses from a laser amplifier are sent through a Michelson interferometer, which introduces a relative delay, thereby leading to a sinusoidal intensity modulation of the recombined pulses. The periodic electron density modulation caused by these pulses results in a narrow emission spectrum.

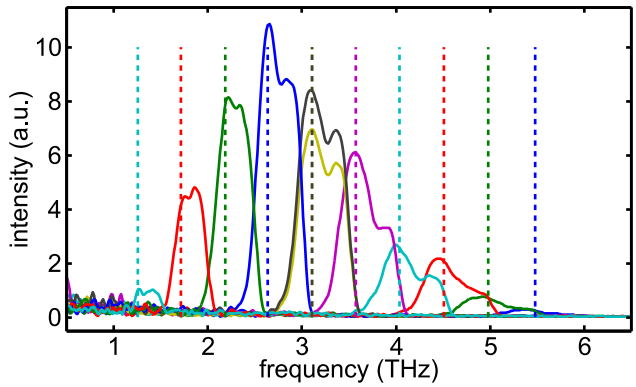

Figure 8: Coherent narrow-band THz spectra, normalized to the bunch current and recorded using different settings of the Michelson interferometer. The modulation frequencies of the laser pulse, measured by an optical autocorrelator, are shown as dashed lines.

In cooperation with the laboratory for laser, atomic and molecular physics PhLAM/CERLA in Lille, pulses with frequencies between 1.3 THz and 5.5 THz and bandwidths between 300 GHz and 650 GHz could be successfully generated at DELTA using 11-ps (FWHM) laser pulses under variation of the delay in the Michelson interferometer (Fig. 8). Studies employing this technique will continue with one application being the investigation of the transition between the bolometric and electric field detection mechanisms of the YBCO detector.

OUTLOOK

Recently, a YBCO detector from IMS has been permanently installed at DELTA, which will allow more regular studies of the turn-by-turn evolution of the laser-induced density modulation. More extensive simulations under variation of machine and laser parameters will be performed. In cooperation with PhLAM/CERLA, it is planned to build a permanent setup at DELTA for routine generation of narrow-band THz radiation. In order to further extend the detectable frequency range, the z-cut quartz window of the THz beamline should be replaced. The commercial FT-IR spectrometer will be complemented by a self-built polarizing Michelson interferometer by the end of 2014 [20, 21].

ACKNOWLEDGMENT

It is a pleasure to thank our colleagues at DELTA and the Faculty of Physics at the TU Dortmund University, ANKA, IMS and IPS at KIT, and PhLAM/CERLA at Lille 1 University for their continuous support. The advice from Karsten Holldack at BESSY/HZB regarding the design, construction, and commissioning of the THz beamline is gratefully acknowledged. Furthermore, the project has profited from the expertise of our colleagues at DESY, MLS/PTB, SLS/PSI, and UVSOR.

REFERENCES

[1] R. Coisson and F. D. Martini, Phys. of Quant. Electron. 9, 939 (1982).

[2] H. Huck et al., Proc. of FEL 2011, Shanghai, 5.

[3] S. Khan et al., Sync. Rad. News 26, No. 3, 25 (2013).

[4] M. Huck et al., this conference (WEOAA03).

[5] K. Holldack et al., Phys. Rev. Lett. 96, 054801 (2006).

[6] M. Höner et al., Proc. of IPAC 2011, San Sebastián, 2939.

[7] P. Ungelenk et al., Proc. of IPAC 2012, New Orleans, 768.

[8] P. Ungelenk et al., Proc. of IPAC 2013, Shanghai, 94.

[9] A. D. Semenov et al., Proc. of IRMMW-THz 2009, 5324688.

[10] A.-S. Müller et al., Proc. of PAC 2009, Vancouver, 1153.

[11] P. Thoma et al., Appl. Phys. Lett. 101, 142601 (2012).

[12] P. Thoma et al., IEEE Trans. Terahertz Sci. Technol. 3, No. 1, 81 (2013).

[13] P. Probst et al., Phys. Rev. B 85, 174511 (2012).

[14] P. Thoma, PhD thesis, Karlsruhe Institute of Technology 2013.

[15] L.-G. Böttger, bachelor's thesis, TU Dortmund 2013.

[16] M. Borland, Advanced Photon Source LS-287 (2000).

[17] S. Bielawski et al., Nature Physics 4, 390 (2008).

[18] C. Evain et al., PRST-AB 13, 090703 (2010).

[19] A. S. Weling and D. H. Auston, J. Opt. Soc. Am. B 13, No. 12, 2783 (1996).

[20] D. H. Martin and E. Puplett, Infrared Physics 10, No. 2, 105 (1970).

[21] C. Mai, master's thesis in preparation, TU Dortmund 2014.

ISBN 978-3-95450-132-8